Hindawi
Journal of Sensors
Volume 2018, Article ID 3019259, 8 pages
https://doi.org/10.1155/2018/3019259

Research Article

Detection of Immunoglobulin E with a Graphene-Based Field-Effect Transistor Aptasensor

Yi Lan,[1] Sidra Farid,[1] Xenia Meshik,[2] Ke Xu,[1] Min Choi,[1] Saadia Ranginwala,[1] Yung Yu Wang,[3] Peter Burke,[4] Mitra Dutta,[1,5] and Michael A. Stroscio[1,2]

[1]*Department of Electrical and Computer Engineering, University of Illinois, Chicago, IL 60607, USA*
[2]*Department of Bioengineering, University of Illinois, Chicago, IL 60607, USA*
[3]*Department of Chemical Engineering and Materials Science, University of California, Irvine, CA 92697, USA*
[4]*Department of Electrical Engineering and Computer Science, University of California, Irvine, CA 92697, USA*
[5]*Department of Physics, University of Illinois, Chicago, IL 60607, USA*

Correspondence should be addressed to Sidra Farid; sidrafarid@gmail.com

Received 5 February 2018; Accepted 28 June 2018; Published 22 July 2018

Academic Editor: Heinz C. Neitzert

DNA aptamers have the ability to bind to target molecules with high selectivity and therefore have a wide range of clinical applications. Herein, a graphene substrate functionalized with a DNA aptamer is used to sense immunoglobulin E. The graphene serves as the conductive substrate in this field-effect-transistor-like (FET-like) structure. A voltage probe in an electrolyte is used to sense the presence of IgE as a result of the changes in the charge distribution that occur when an IgE molecule binds to the IgE DNA-based aptamer. Because IgE is an antibody associated with allergic reactions and immune deficiency-related diseases, its detection is of utmost importance for biomedical applications.

1. Introduction

Allergic reactions and allergic conditions have a significant impact on a person's health that have become the leading cause of chronic illness globally. Especially in the United States, allergies are the sixth leading cause of chronic illness causing millions of Americans to suffer from such allergies annually [1, 2]. Young children and infants in their early life are exposed to a variety of environmental allergens that may generate or simulate an immune response. Allergic triggers may include food, insect stings, environmental factors, chemicals, or a condition of strong family history of atopy; however, the response often includes production of an immunoglobulin E (IgE) antibody [3]. These antibodies are a major component of the body's immune system that can help fight antigens like viruses, bacteria, and fungi that are believed to be harmful to the body [4].

Various tests such as blood, skin, serological, or radioallergosorbent tests are traditionally used for the detection of IgE-mediated allergy testing [5, 6]. However, a positive test alone is not sufficient to diagnose an allergic condition. A sensitization may be determined from these tests, but they may not always indicate the clinical reactivity. This requires chemical/thermal stability and selective sensing of target molecules [7]. In this study, we have used aptamers as a receptor molecule that has the ability to bind to the specific target molecules and can selectively detect only the target protein. Their ease of modification, enhanced chemical and thermal stability, and ability to denaturalize under unfavorable conditions make them a viable candidate for biomedical sensing applications [8, 9].

Field-effect-transistor- (FET-) like structures incorporating graphene substrates and DNA aptamer molecular

sensing elements have been used to detect small molecules and ions of physiological interest [10]. In the past, we have successfully demonstrated detection of K^+ and Pb^{2+} ions, cytokines such as interferon-gamma (IFN-γ), and adenosine monophosphate (AMP) with graphene-based platforms [11–13]. Graphene has an extremely high carrier mobility, large sheet carrier concentration, and unique ambipolar characteristics that make it a suitable candidate for biomolecular sensing [14]. However, for the detection of heavy metal ions, the thrombin-binding aptamer (TBA) functionalized to the graphene layer was used, which undergoes a conformational change and binds to the aptamer on the introduction of target ions [15].

In this study, immunoglobulin E (IgE) aptamer and a liquid-gate FET structure are used to detect IgE protein, and detection is achieved due to the changes in charge distribution in the electrolyte, which occurs upon binding of IgE to the IgE aptamer. This change in charge distribution causes a current change across graphene that is found to be dependent on the concentrations of IgE. Such sensitive and simple graphene-based electrochemical nanobiosensor has potential applications in the diagnosis of allergies, immunosensing, and can be an effective analytical tool for biomedical applications.

2. Experiments

2.1. Fabrication of a Monolayer Graphene-Based Field-Effect Transistor. Monolayer graphene-based liquid-gated FET-like transistors were fabricated at the University of California, Irvine by Yung Yu Wang and are described in detail in their previous work [16]. A step-by-step fabrication protocol is described in the schematic shown in Figure 1. As described, monolayer graphene was fabricated on a Cu foil using the chemical vapor deposition (CVD) process and attached on a polydimethylsiloxane (PDMS) substrate. Raman investigations were carried out using a Renishaw Raman microscope with an excitation input of 514 nm. Monolayer graphene peaks were detected after mapping at various spots on the graphene surface. Structural verification was done using scanning electron microscopy (SEM) and atomic force microscopy (AFM), which shows a contamination- and crack-free monolayer graphene layer.

After the verification of the graphene layer, the Cu foil is etched away and the PDMS/graphene structure was rinsed several times with DI water. In order to hold the electrolyte solution in it, a second PDMS layer is attached onto the graphene platform. This creates a well that is capable of carrying the electrolyte and holds the liquid-gated probe. Source and drain electrodes for the FET-like structures are formed at both ends of the graphene layer using silver paint. The circuit configuration for the graphene-based FET is shown in Figure 2 where the graphene serves as a conducting substrate between the drain and source terminals.

2.2. Primary Device Characteristic Testing. In order to ensure good contact between the channels, device output characteristics using current-voltage relation are measured before the functionalization of DNA aptamers using an Agilent Semiconductor Parameter Analyzer. The I_{DS} versus V_{DS} curve is obtained for checking the conductivity between drain and source terminals. This is done after filling the well of the structure with 1x phosphate-buffered saline (PBS). The graph appears to be a straight line showing good conductivity of monolayer graphene between its two sources and drain terminals, whereas the slope of the linear plot determines the resistance between drain and source terminals.

For checking the functionality of the graphene layer, the device transfer characteristic is taken by measuring drain current versus gate voltage keeping V_{DS} constant. A flexible microreference Ag/AgCl electrode with a 1 mm tip was purchased from Microelectrodes Inc. (Bedford, NH). The glass filament is filled with 3 M KCl solution, and the tip of the electrode is placed in the well to apply the gate voltage. The graph shows ambipolar field-effect transfer-like behavior identifying good quality samples, which can be used for the remainder of the experiments.

2.3. Aptamer Selection. The DNA-based sequence of IgE aptamer was made analytically and chosen based on literature studies as presented in Table 1. A stable tertiary structure of IgE aptamer (5′-pyrene-GCG C GGGG CACG TTTA TCCG T CCC TCCTAGTGGCGTGCCCC GCGC-3′) is chosen with a modification of 5′-GCGC-3′ sequences being added to extend both the 5′ and 3′ ends.

The pyrene group on the 5′ enables the aptamer to bind to the graphene surface. By implementing this process, the dissociation constant of the IgE aptamer was reduced to 3.6 nm, and this improved its binding characteristics. Also, the fact that many different studies have demonstrated the effectiveness of this particular sequence led to its selection in our work. Aptamer (5′-pyrene-GCG C GGGG CACG TTTA TCCG T CCC TCCTAGTGGCGTGCCCC GCGC-3′) was purchased from Biosearch Technologies (Novato, CA).

2.4. Binding Aptamer on Monolayer Graphene. In order to bind the aptamer to the graphene surface, a 20 μL drop of 250 μM aptamer in anhydrous DMF (dimethylformamide) is dropped in the well and left to incubate for 3 hours. The well is then washed three times with 1x PBS and filled with 60 μL of PBS after washing. The gate electrode is placed in the well such that the tip is submerged in PBS but does not touch the bottom. I_{DS}-V_G curves are then obtained.

Human myeloma plasma IgE was purchased from Athens Research & Technology (Athens, GA) and dissolved in deionized H_2O to a concentration of 1 μM. The IgE solution is added to the well in 5 μL drops and left to sit for 2 minutes for the IgE molecule to distribute uniformly, and the I_{DS}-V_G curve is tested again. Care must be taken in order not to shift the gate electrode because this might cause a change in resistance from drain/source to gate. To have all experimental data normalized,

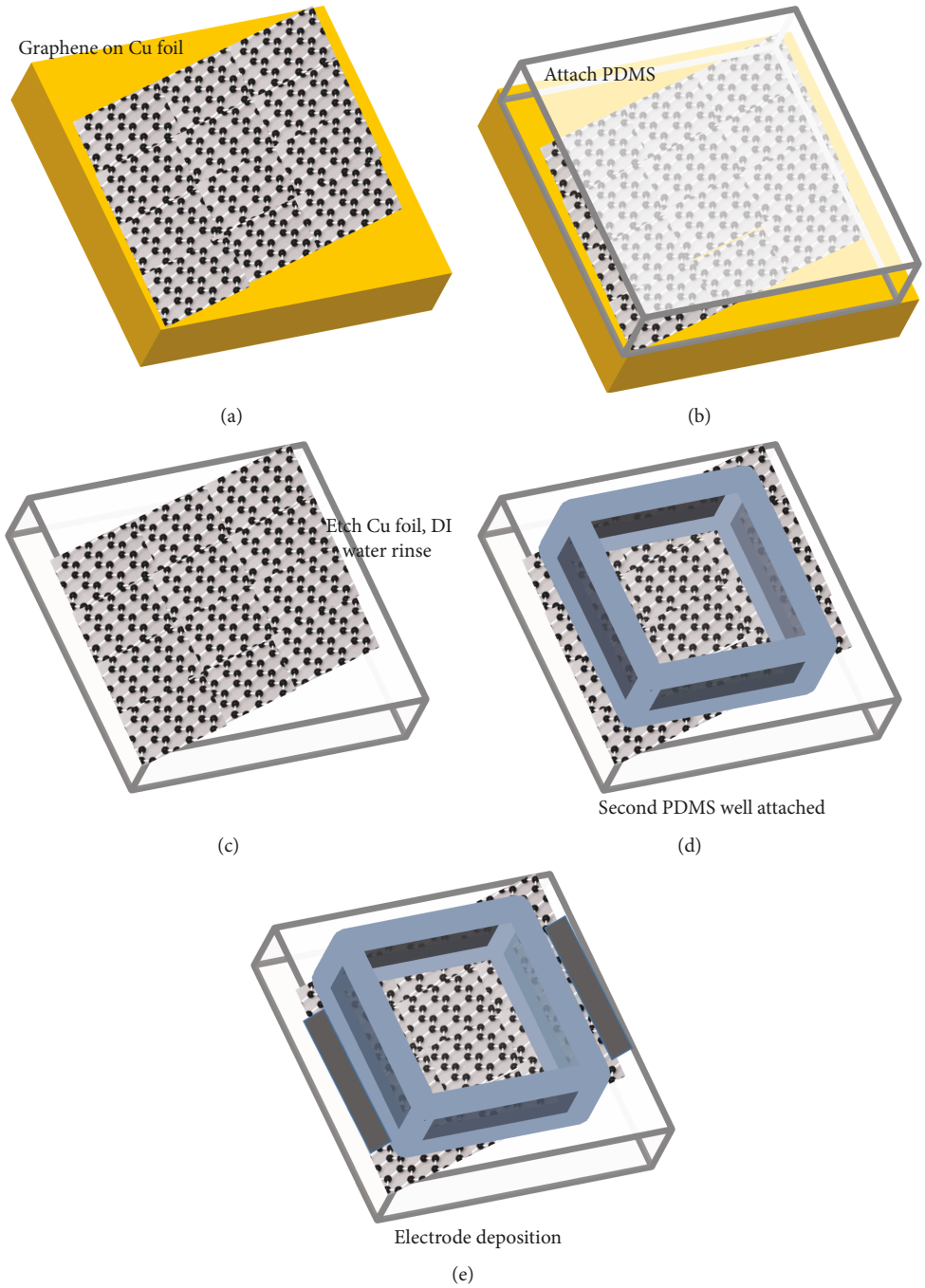

Figure 1: Fabrication steps for a graphene film transferred onto the PDMS substrate.

the position of the gate cannot be changed while obtaining the I_{DS}-V_G curves for all different concentrations on one sample.

3. Results and Discussions

3.1. Electrochemical Detection of IgE. The IgE aptamer is attached onto the graphene surface, and 5 μL of 1 μM IgE solution is added in turn into the well containing PBS while keeping V_{DS} constant at 0.3 V. Device transfer characteristics are measured, and I_{DS}-V_G data for different concentrations of IgE are recorded. As shown in Figure 3, it is seen that as the concentration of IgE is increased, a dynamic enhancement in current is noticed. The current increases by about 10^{-7} mA after each addition of 5 μL of 1 μM IgE. This change in current could be the result of the introduction of charge carriers on the addition of target ions resulting in a change of conductivity in the proposed aptasensor. This increases the electron current efficiency that provides the basis for detection for target molecules. It is also worth noting that there is no significant shift in the Dirac point which is the minimum

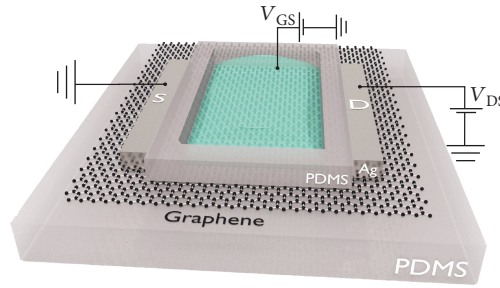

Figure 2: Schematic diagram for a graphene-based FET-like electrochemical biosensor.

Table 1: IgE aptamer selection from literature survey.

	IgE aptamer	Reference
(1)	5′-NH2-GCG C GG GGC ACG TTT ATC CGT CCC TCC TAG TGG CGT GCC CCG CGC-3′	[17]
(2)	5′-NH2-GCG C GG GGC ACG TTT ATC CGT CCC TCC TAG TGG CGT GCC CCG CGC-3′	[18]
(3)	5′-SH-GGG GCA CGT TTA TCC GTC CCT CCT AGT GGC GTG CCC C-3′	[19]
(4)	5′-SH-GGG GCA CGT TTA TCC GTC CCT CCT AGT GGC GTG CCC C-3′	[20]
(5)	5-NH2-GCG C GGGG CACG TTTA TCCG T CCC TCCTAGTGGCGTGCCCC GCGC-3	[21]

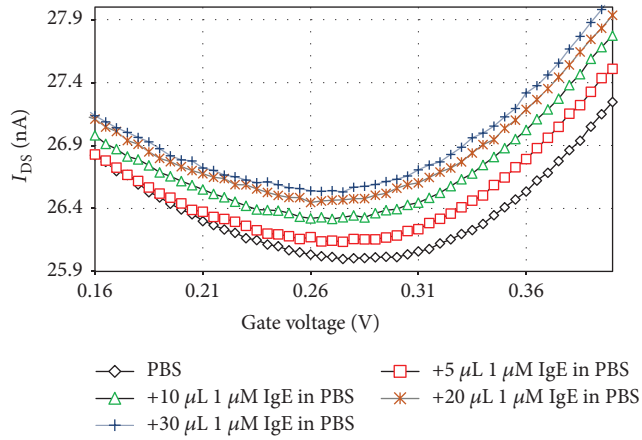

Figure 3: I_{DS}-V_G curve for FET-like sensor structure with IgE aptamer attached onto the monolayer graphene after adding different IgE concentrations into the well.

Table 2: I_0, V_{Dirac}, and minimum conduction current at different concentrations of IgE.

Volume of 1 μM IgE in PBS	I_0 (nA)	V_{Dirac} (V)	Minimum conduction current (nA)
0 μL	29.334	0.275	25.998
5 μL	29.299	0.275	26.135
10 μL	29.466	0.270	26.316
15 μL	29.505	0.275	26.368
20 μL	29.636	0.260	26.448
25 μL	29.693	0.255	26.503
30 μL	29.732	0.265	26.536

conductance point in the device transfer curve, which indicates that the *n*- or *p*-type property of the graphene does not change with IgE [22]. The volume of IgE in PBS, initial current (I_0) (when no gate voltage is applied), Dirac voltage, and minimum conduction current are shown in Table 2.

3.2. Selectivity of the IgE Sensor. The selectivity of this aptamer has been tested against other ions such as those used by Salimi et al. and Cole et al., and those results are taken into consideration in this study [23, 24]. Additionally, two sets of control experiments were investigated in order to confirm the stability and selectivity of the proposed sensor. For the first set, 5 μL drops of 1 μM bovine

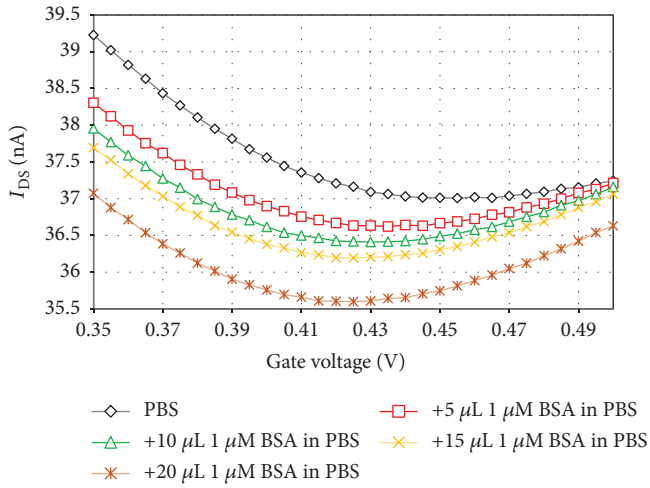

Figure 4: I_{DS}-V_G curve for FET-like sensor structure with IgE aptamer attached onto the monolayer graphene after adding different BSA concentrations into the well.

Table 3: I_0, V_{Dirac}, and minimum conduction current at different concentrations of BSA.

Capacity of 1 μM BSA in PBS	I_0 (nA)	V_{Dirac} (V)	Minimum conduction current (nA)
0 μL	53.950	0.455	37.007
5 μL	53.272	0.445	36.629
10 μL	53.019	0.430	36.408
15 μL	53.333	0.425	36.194
20 μL	53.227	0.425	35.598

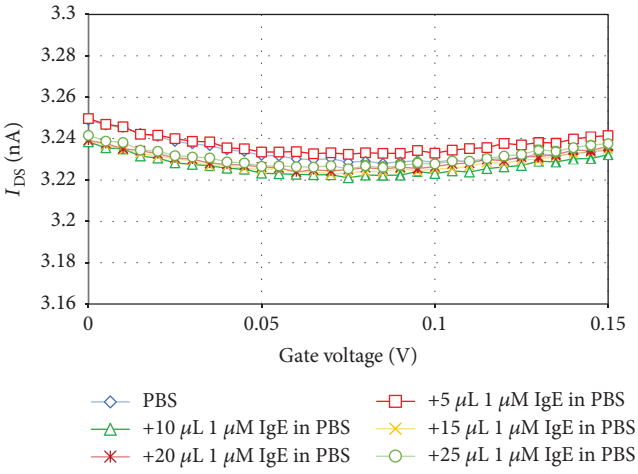

Figure 5: I_{DS}-V_G curve for FET-like sensor structure with no aptamer attached onto the monolayer graphene after adding different IgE concentrations into the well.

serum albumin (BSA) which is another nonspecific protein are added to the aptamer-functionalized well instead of IgE. Device transfer characteristics are measured again keeping the drain voltage and target concentrations the same as in the previous sensor experiment. As shown in

Table 4: I_0, V_{Dirac}, and minimum conduction current at different concentrations of IgE with no aptamer attached on the monolayer graphene.

Volume of 1 μM IgE in PBS	I_0 (nA)	V_{Dirac} (V)	Minimum conduction current (nA)
0 μL	3.2489	0.075	3.2286
5 μL	3.2497	0.075	3.2324
10 μL	3.2384	0.075	3.2211
15 μL	3.2391	0.070	3.2227
20 μL	3.2392	0.070	3.2244
25 μL	3.2416	0.075	3.2254

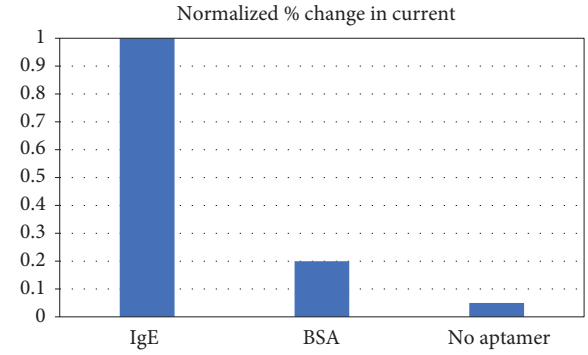

Figure 6: Normalized percent change in current at the same concentration values (20 μL) for all target and nontarget proteins at the Dirac point.

Figure 4, as the concentration of BSA increases, I_{DS} went down, which implies that BSA in solution has a negative effect on current conduction and the rate at which current changes is larger as compared to when IgE target is added. The current decreases after each addition of 5 μL of 1 μM BSA, as depicted in Table 3. Again, the change of V_{Dirac} is

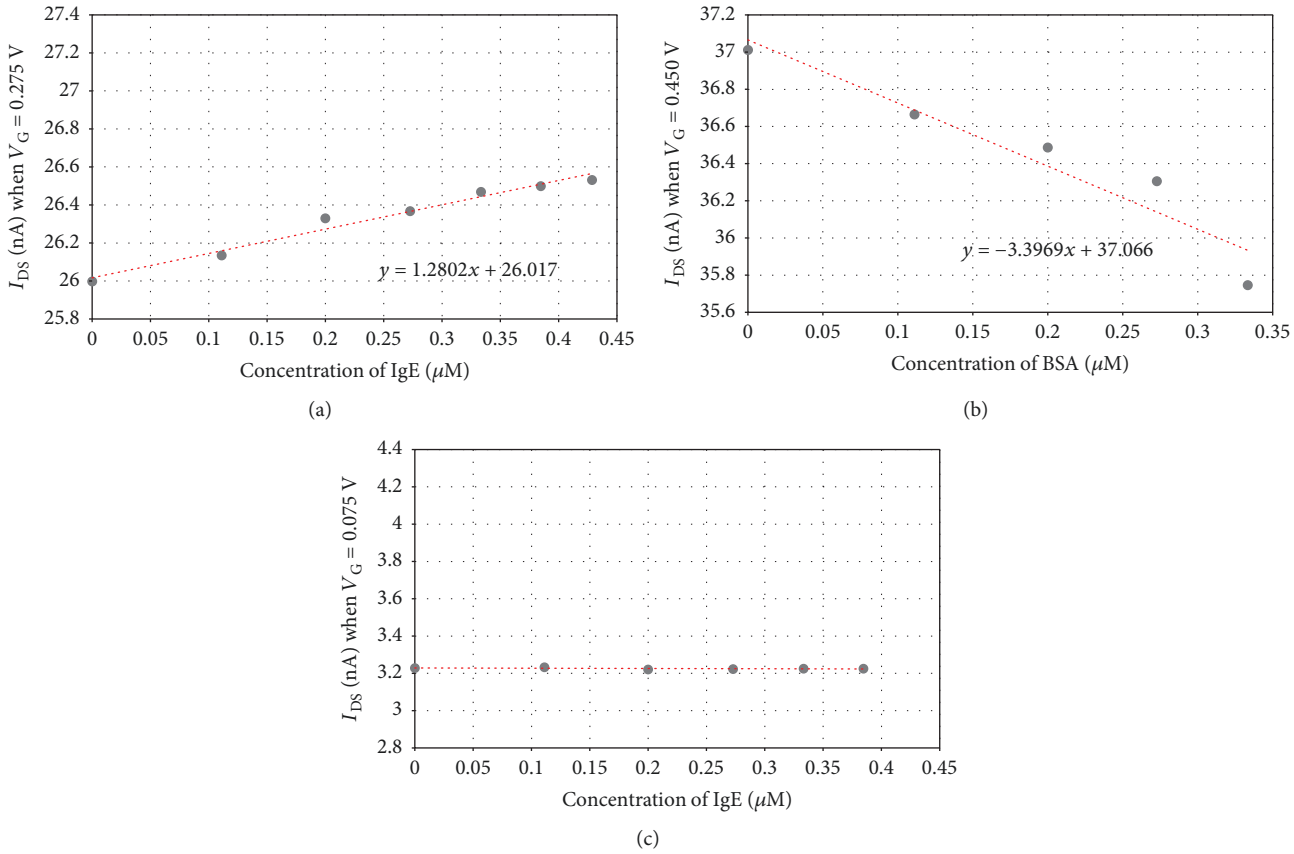

Figure 7: The regression lines of I_{DS} versus concentrations of (a) IgE, (b) BSA, and (c) no target.

minimal. The slight shift in the Dirac point is the result of the *p*-type doping effect due to the charge carrier induction. It is also concluded that the IgE aptamer bound on the graphene FET-like sensor can also be a good apparatus for testing BSA targets. BSA targets might have the ability to repel IgE aptamers and reduce its conductivity in solvent, which could itself be a study for future investigations.

After testing the ability of IgE aptamer to distinguish IgE and BSA target molecules, another control experiment is performed by adding 5 μL drops of 1 μM IgE target to samples with no IgE aptamer. As shown in Figure 5, the curve is nearly unaffected by increasing target concentration, and the current does not consistently increase or decrease compared to sensor experiments. I_0, V_{Dirac}, and minimum conduction current at different concentrations of IgE with no aptamer attached on the monolayer graphene are depicted clearly in Table 4. This change in current in response to target and nontarget proteins is also depicted in Figure 6 for the same concentration values. Such lack of response from control experiments as compared to the proposed sensor experiment reveals that a graphene-based biosensor can actively detect IgE with high sensitivity.

3.3. Relationship between Current and IgE Concentration. The relation between current and IgE concentration is estimated for calculating the sensitivity of our sensor. Current I_{DS} versus concentration of IgE is plotted at a constant gate voltage near the Dirac point. For the graph in Figure 7(a), a positive relationship can be seen between I_{DS} and the concentrations of IgE. The slope of the regression line is the change of I_{DS} corresponding to the change in IgE concentration, which can be found as $\Delta I_{DS}/\Delta\text{Concentration} \approx 1.2902$ (nA/μM). In the case of I_{DS} versus concentration of BSA, a negative trend line is shown in Figure 7(b), which indicates that when the concentration of BSA is increased, the I_{DS} current will decrease. The correlation can be described as $\Delta I_{DS}/\Delta\text{Co ncentration} \approx -3.3969$ (nA/μM), whereas no relationship between I_{DS} and the concentration of IgE can be found in the control experiment with no aptamer on the graphene surface. Thus, the sensor could detect the IgE molecule with only a small voltage across drain and source, along with added advantage of requiring extremely small sample volume i–e ~ 1 μL or less, which makes it more applicable for detecting small analytes in the future.

4. Conclusions

We have successfully designed a graphene-based FET-like electrochemical biosensor for detecting IgE target molecules. Detection is achieved by taking advantage of highly conductive properties of a graphene platform that causes an increase in electron current efficiency on the addition of IgE target molecules. Control experiments were

performed to reveal the stability and selectivity of the proposed biosensor that indicate that the sensor is highly selective to IgE target molecules. Thus, the proposed detection mechanism of the IgE antibody will be of utmost importance for diseases related to allergic reactions or immune deficiency and would be useful for biomedical applications.

Data Availability

The data used to support the findings of this study are available from the corresponding author upon request.

Disclosure

Sidra Farid's current address is the Department of Electrical Engineering, University of Engineering and Technology, Lahore, Pakistan.

Conflicts of Interest

The authors declare that they have no conflicts of interest.

Acknowledgments

This work was supported by ARO through MURI Grant W911NF-11-1-0024. Support through the Richard and Loan Hill Professorship is also acknowledged.

References

[1] A. A. Cruz, *Global Surveillance, Prevention and Control of Chronic Respiratory Diseases: A Comprehensive Approach*, World Health Organization, 2007.

[2] M. Masoli, D. Fabian, S. Holt, and R. Beasley, "The global burden of asthma: executive summary of the GINA dissemination committee report," *Allergy*, vol. 59, no. 5, pp. 469–478, 2004.

[3] S. Rowntree, J. J. Cogswell, T. A. Platts-Mills, and E. B. Mitchell, "Development of IgE and IgG antibodies to food and inhalant allergens in children at risk of allergic disease," *Archives of Disease in Childhood*, vol. 60, no. 8, pp. 727–735, 1985.

[4] J. Dolovich, F. E. Hargreave, R. Chalmers, K. J. Shier, J. Gauldie, and J. Bienenstock, "Late cutaneous allergic responses in isolated IgE-dependent reactions," *Journal of Allergy and Clinical Immunology*, vol. 52, no. 1, pp. 38–46, 1973.

[5] B. Burrows, F. D. Martinez, M. Halonen, R. A. Barbee, and M. G. Cline, "Association of asthma with serum IgE levels and skin-test reactivity to allergens," *The New England Journal of Medicine*, vol. 320, no. 5, pp. 271–277, 1989.

[6] L. Guilloux, S. Ricard-Blum, G. Ville, and J. Motin, "A new radioimmunoassay using a commercially available solid support for the detection of IgE antibodies against muscle relaxants," *Journal of Allergy and Clinical Immunology*, vol. 90, no. 2, pp. 153–159, 1992.

[7] D. P. Skoner, "Allergic rhinitis: definition, epidemiology, pathophysiology, detection, and diagnosis," *Journal of Allergy and Clinical Immunology*, vol. 108, no. 1, pp. S2–S8, 2001.

[8] D. Datta, X. Meshik, S. Mukherjee et al., "Submillimolar detection of adenosine monophosphate using graphene-based electrochemical aptasensor," *IEEE Transactions on Nanotechnology*, vol. 16, no. 2, pp. 196–202, 2017.

[9] X. Meshik, S. Farid, M. Choi et al., "Biomedical applications of quantum dots, nucleic acid– based aptamers, and nanostructures in biosensors," *Critical reviews™ in Biomedical Engineering*, vol. 43, no. 4, pp. 277–296, 2015.

[10] K. Xu, M. Purahmad, K. Brenneman et al., "Design and applications of nanomaterial-based and biomolecule-based nanodevices and nanosensors," in *Design and Applications of Nanomaterials for Sensors*, J. Seminario, Ed., vol. 16 of Challenges and Advances in Computational Chemistry and Physics, pp. 61–97, Springer, Dordrecht, 2014.

[11] X. Meshik, K. Xu, M. Dutta, and M. A. Stroscio, "Optical detection of lead and potassium ions using a quantum-dot-based aptamer nanosensor," *IEEE Transactions on Nanobioscience*, vol. 13, no. 2, pp. 161–164, 2014.

[12] S. Farid, X. Meshik, M. Choi et al., "Detection of interferon gamma using graphene and aptamer based FET-like electrochemical biosensor," *Biosensors and Bioelectronics*, vol. 71, pp. 294–299, 2015.

[13] S. Mukherjee, X. Meshik, M. Choi et al., "A graphene and aptamer based liquid gated FET-like electrochemical biosensor to detect adenosine triphosphate," *IEEE Transactions on Nanobioscience*, vol. 14, no. 8, pp. 967–972, 2015.

[14] J. D. Fowler, M. J. Allen, V. C. Tung, Y. Yang, R. B. Kaner, and B. H. Weiller, "Practical chemical sensors from chemically derived graphene," *ACS Nano*, vol. 3, no. 2, pp. 301–306, 2009.

[15] K. L. Brenneman, S. Poduri, M. A. Stroscio, and M. Dutta, "Optical detection of lead (II) ions using DNA-based nanosensor," *IEEE Sensors Journal*, vol. 13, no. 5, pp. 1783–1786, 2013.

[16] Y. Yu Wang and P. J. Burke, "A large-area and contamination-free graphene transistor for liquid-gated sensing applications," *Applied Physics Letters*, vol. 103, no. 5, article 052103, 2013.

[17] K. Maehashi, T. Katsura, K. Kerman, Y. Takamura, K. Matsumoto, and E. Tamiya, "Label-free protein biosensor based on aptamer-modified carbon nanotube field-effect transistors," *Analytical Chemistry*, vol. 79, no. 2, pp. 782–787, 2007.

[18] Y. Ohno, K. Maehashi, and K. Matsumoto, "Label-free biosensors based on aptamer-modified graphene field-effect transistors," *Journal of the American Chemical Society*, vol. 132, no. 51, pp. 18012-18013, 2010.

[19] D. Xu, D. Xu, X. Yu, Z. Liu, W. He, and Z. Ma, "Label-free electrochemical detection for aptamer-based array electrodes," *Analytical Chemistry*, vol. 77, no. 16, pp. 5107–5113, 2005.

[20] Z. Wang, T. Wilkop, D. Xu, Y. Dong, G. Ma, and Q. Cheng, "Surface plasmon resonance imaging for affinity analysis of aptamer–protein interactions with PDMS microfluidic chips," *Analytical and Bioanalytical Chemistry*, vol. 389, no. 3, pp. 819–825, 2007.

[21] S. Khezrian, A. Salimi, H. Teymourian, and R. Hallaj, "Label-free electrochemical IgE aptasensor based on covalent attachment of aptamer onto multiwalled carbon nanotubes/ionic liquid/chitosan nanocomposite modified electrode," *Biosensors and Bioelectronics*, vol. 43, pp. 218–225, 2013.

[22] K. Xu, X. Meshik, B. M. Nichols, E. Zakar, M. Dutta, and M. A. Stroscio, "Graphene-and aptamer-based electrochemical biosensor," *Nanotechnology*, vol. 25, no. 20, article 205501, 2014.

[23] A. Salimi, S. Khezrian, R. Hallaj, and A. Vaziry, "Highly sensitive electrochemical aptasensor for immunoglobulin E detection based on sandwich assay using enzyme-linked aptamer," *Analytical Biochemistry*, vol. 466, pp. 89–97, 2014.

[24] J. R. Cole, L. W. Dick, E. J. Morgan, and L. B. McGown, "Affinity capture and detection of immunoglobulin E in human serum using an aptamer-modified surface in matrix-assisted laser desorption/ionization mass spectrometry," *Analytical Chemistry*, vol. 79, no. 1, pp. 273–279, 2007.